Int. J. Multiphase Flow, Vol. 3, pp. 501–515. Pergamon/Elsevier, 1977. Printed in Great Britain

THE CALCULATION OF DRYOUT IN A ROD BUNDLE

P. B. WHALLEY
Thermodynamics Division, A.E.R.E. Harwell, Oxon, U.K.

(*Received* 4 *October* 1976; *received for publication* 24 *May* 1977)

Abstract—A model of annular two-phase flow is used to calculate dryout on the assumption that dryout occurs when the liquid flowrate in the film on the solid surfaces becomes equal to zero. To enable the calculation to be performed, the processes of entrainment and deposition of liquid droplets must be adequately described. The rod bundle is divided, for calculational purposes, into rod centred subchannels, and the liquid flows in the liquid films and as droplets in each subchannel are calculated. The agreement between experiment and calculation for dryout power is encouraging.

1. INTRODUCTION

If water is boiled in the core of a nuclear reactor, the power which can be generated in each rod containing the nuclear fuel is often limited by the power at which the surface of the rod will not be wetted by water. If the above limit is reached the coefficient for heat transfer from the rod drops very dramatically, and the rod temperature may be unacceptably high. This phenomenon of dryout, or burnout, has been studied for many years in round tubes as well as in geometries more appropriate to a nuclear reactor. It has been found that when dryout occurs, it is often associated with a particular type of gas–liquid two phase flow, namely annular flow (see figure 1). The flow regimes which are commonly reached before annular flow are shown in figure 1 for flow in a tube. Flow regimes in rod bundles have received comparatively little attention, but Bergles *et al.* (1968) and Williams & Peterson (1975) have found that, for the flow of steam–water mixtures in rod bundles at a pressure of approximately 70 bars, the same flow regimes occur.

The essential features of annular flow are that the gas travels in the centre of the channel, a liquid film travels on the channel walls and liquid drops are carried along with the gas flow. These droplets are continually torn off the liquid film, most probably from large disturbance waves on the liquid film, and are subsequently redeposited onto the film again. Further details of annular flow are given by Hewitt & Hall Taylor (1970). When dryout is associated with annular flow it has been found by Hewitt *et al.* (1965) that the film flow rate approaches zero smoothly, and that the point where it becomes equal to zero is the point where dryout occurs. This smooth decay of the film flowrate to zero suggests that with an annnular flow model containing some description of the entrainment and deposition processes, it ought to be possible to calculate the position of dryout for a given heat flux, or the lowest heat flux that will give dryout at any point. Such a model was found to give reasonable results for calculations of this type for flow in a round tube (Whalley *et al.* 1974) and for flow in an annulus (Whalley *et al.* 1975). The present work extends the analysis to an array of vertical rods.

Computer programs such as HAMBO (Bowring 1967, 1968) and COBRA (Rowe 1967, 1970, 1972, 1973) divide the array of rods into subchannels, see figure 2, and then apply the assumptions of homogeneous or separated flow to the two phase flows in these subchannels. As has been noted by Weisman & Bowring (1975) such subchannels are not suitable for use with an annular flow model, the rod-centred subchannels first used by Gaspari *et al.* (1970, 1974), see figure 3, are more suitable. This is because such subchannels do not contain solid surfaces from more than one rod, possibly having different heat fluxes. Butterworth (1968) has shown that the film flowrate, though not the film thickness, around a rod is reasonably uniform even when the rod is placed eccentrically inside a tube. To a first approximation the liquid film flow rate can therefore be assumed to be constant around a rod in a rod bundle.

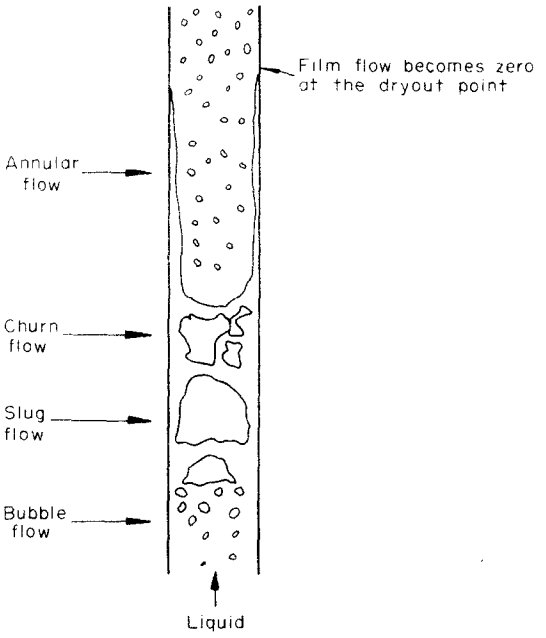

Figure 1. Two-phase flow regimes during vertical flow in a heated tube.

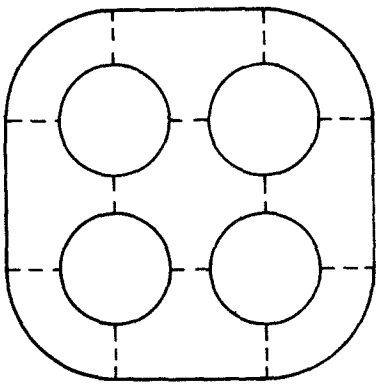

Figure 2. Conventional subchannels.

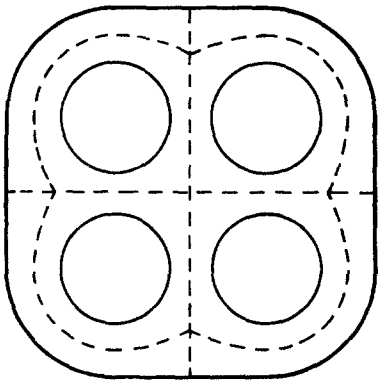

Figure 3. Rod centred subchannels.

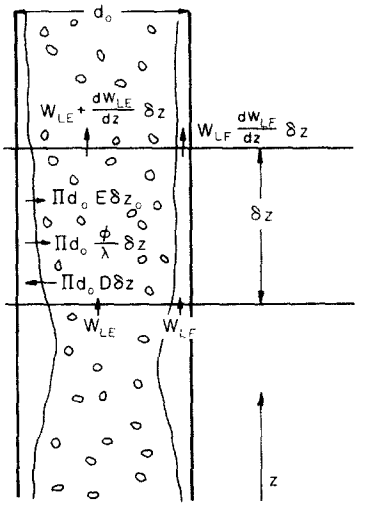

Figure 4. Mass balance of entrained liquid flow and film flow in a single round tube.

The application of an annular flow model to the calculation of critical heat flux is first presented for a round tube, and then extended to the rod bundle geometry.

2. DRYOUT IN A SINGLE ROUND TUBE

2.1 *Basic equations*

In figure 4, the mass flowrates between the liquid film, the entrained liquid drops, and the gas (or vapour) are shown for an elemental length δz. By performing mass balances on the liquid

film and on the entrained liquid flow, it can easily be shown that

$$\frac{dW_{LE}}{dz} = \pi d_0(E - D), \quad [1]$$

$$\frac{dW_{LF}}{dz} = \pi d_0 \left(D - E - \frac{\phi}{\lambda}\right) \quad [2]$$

where

W_{LE} is the mass flowrate of entrained liquid droplets;
W_{LF} is the mass flowrate in the liquid film;
z is the axial co-ordinate in the direction of flow;
d_0 is the diameter of the tube;
D is the deposition rate of droplets onto the liquid film;
E is the entrainment rate of droplets from the liquid film;
ϕ is the heat flux through the walls of the tube;
and
λ is the latent heat of vaporisation of the liquid.

Although two equations are given here, [1] and [2], together they simply express an overall mass balance on the liquid phase, for adding the equations

$$\frac{dW_L}{dz} = -\frac{\pi d_0 \phi}{\lambda} \quad [3]$$

where W_L is the total mass flowrate of liquid at any axial point z.

Before [1] and [2] can be integrated, methods must be available for calculating the deposition and entrainment rates, D and E.

2.2 *Deposition rate*

It has been found by Cousins *et al.* (1965) and Cousins & Hewitt (1968) that the deposition can be characterised by a mass-transfer coefficient k such that

$$D = kC \quad [4]$$

where C is the concentration of entrained droplets. This concentration is calculated from the assumption that there is no relative velocity between the liquid drops and the gas, so that

$$C = \frac{W_{LE}}{\frac{W_{LE}}{\rho_L} + \frac{W_G}{\rho_G}}, \quad [5]$$

where W_G is the mass flowrate of gas;
ρ_G is the gas density, and
ρ_L is the liquid density.

The deposition coefficient, k, has been measured for the case of steam–water flow at a pressure of 69 bars by Bennett *et al.* (1967) who found an average value of 0.01 m/sec. Values of the deposition coefficient for other systems have been estimated by fitting dryout data to results for dryout calculated using the method presented here, and by Whalley *et al.* (1974). The

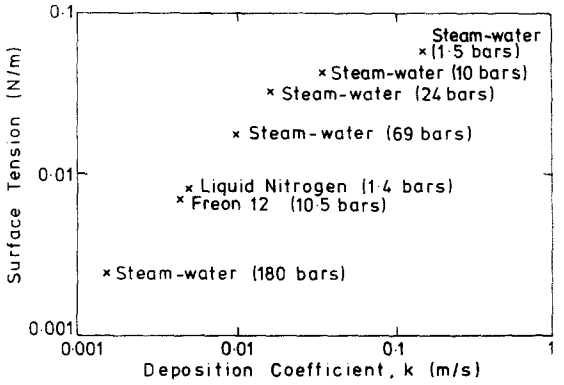

Figure 5. Variation of deposition coefficient with surface tension.

experimental and calculated results for the deposition coefficient are plotted against surface tension in figure 5. From figure 5 it can be seen that

(i) A relationship of the type

$$k = f(\sigma) \qquad [6]$$

where σ is the surface tension, can be formulated.

(ii) The value for k of 0.15 m/sec for a low pressure steam–water system shown in figure 5 is the same as that obtained by Cousins & Hewitt (1968) for a low pressure air–water system.

The factors governing the variation of k are complex and [6] can only be regarded as tentative.

2.3 *Entrainment rate*

Hutchinson & Whalley (1973) suggested that the equilibrium concentration droplets in an annular flow, C_E is given by

$$C_E = f\left(\frac{\tau m}{\sigma}\right) \qquad [7]$$

where τ is the interfacial shear stress and m is the average liquid film thickness. Here, by the term 'equilibrium' is meant the state, which can almost be reached in an adiabatic flow in a long tube, when the entrainment and deposition rates are equal

The relationship corresponding to [7] which was used here is illustrated in figure 6, together with the data points. The data used are drawn from the following sources

(i) the air–water experiments of Gill *et al.* (1964), Truong Quang Minh & Huyghe (1965), Cousins *et al.* (1965), Cousins & Hewitt (1968*a*, 1968*b*), and Gill *et al.* (1969).

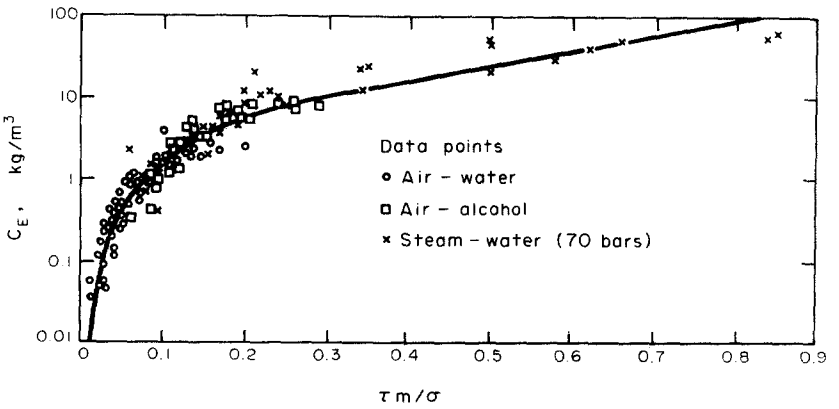

Figure 6. Variation of equilibrium concentration of entrained droplets with $\tau m/\sigma$. (Some data points have been omitted for clarity).

(ii) the air–alcohol experiments of Truong Quang Minh and Huyghe (1965)
(iii) the steam–water experiments of Singh *et al.* (1969) and Keeys *et al.* (1970) at a pressure of 69 bars.

In many cases the data did not include experimentally measured film thicknesses: in these cases the film thickness was calculated using the 'triangular relationship' (see below). In the case of the experiments of Singh *et al.* (1969) no measurements were made of pressure gradient, and so the pressure gradients were estimated by interpolating between the results given by Berkowitz *et al.* (1960) and Janssen & Kervinen (1964).

The rate of entrainment is then obtained by the simple relationship

$$E = kC_E. \qquad [8]$$

This is certainly true at equilibrium (when $E = D$, $D = kC$ and $C = C_E$), and away from equilibrium it is assumed to be true.

To calculate the entrainment rate it is necessary to know the interfacial shear stress and the film thickness. These two quantities can be calculated because if the film flowrate is known there are two relations between them.

(i) A 'triangular relationship'. This is based on the assumption of some known velocity profile in the liquid film, from which it follows that the interfacial shear stress and the film thickness are related. The particular form of triangular relationship used here was one due to Turner & Wallis (1965) and Armand (1946)

$$\frac{4m}{d_0} = \sqrt{\left(\frac{(\mathrm{d}P/\mathrm{d}z)_{LF}}{\mathrm{d}P/\mathrm{d}z}\right)} \qquad [9]$$

where $(\mathrm{d}P/\mathrm{d}z)_{LF}$ is the pressure gradient which would occur in a single phase liquid flow where the mass flow was identical with that in the film, and $\mathrm{d}P/\mathrm{d}z$ is the pressure gradient in the two phase flow. $(\mathrm{d}P/\mathrm{d}z)_{LF}$ was calculated from the liquid film friction factor which is plotted against Reynolds number of Hewitt & Hall Taylor (1970) from numerical data of Hewitt (1961).

(ii) An interfacial roughness correlation. This is based on the assumption that the roughness presented by the liquid film is a function only of the film thickness. The particular form of interfacial roughness correlation used here was due to Wallis (1970), in which the interfacial friction factor (defined in terms of a homogeneous gas core) can be expressed as $(1 + 360m/d_0)$ times the friction factor for the gas core flowing in the absence of the liquid film.

2.4 *Boundary conditions*

The calculation was started at the point in the tube where the quality was equal to 1%, and it was generally found that the best results were produced if it was assumed that 99% of the liquid phase was entrained when the calculation was started. It should be noted that Bennett *et al.* (1965) found that typically annular flow was reached at a quality of 10% in steam–water flow at a pressure of 69 bars. However the calculation is started at a quality of 1%, because the equations used would be expected to have some calculational validity, even though hydrodynamically another flow regime, such as slug flow, may be more stable. It is also found that the results of the calculation are not very sensitive to the boundary conditions as long as the length of the tube over which boiling takes place is not very small. Typically for boiling water flow at a pressure of 69 bars in a tube of diameter 12.6 mm, the effect of the boundary conditions becomes undetectable for boiling lengths greater than about 1 m.

2.5 *Integration method*

It was found that a simple explicit integration scheme required unacceptably short steps in the z direction to give results of reasonable accuracy. An implicit technique was thus found to

be necessary. The integration was continued until the liquid film flowrate became zero when it was assumed that dryout occurred, or until the end of the tube was reached. The critical heat flux is then the lowest value of the heat flux which will cause dryout to occur in the tube. The general scheme of the calculation is explained in more detail for the rod bundle case in section 3.6.

3. DRYOUT IN A ROD BUNDLE

3.1 *Basic equations*

The differential equations for the liquid film flow rate and for the entrained liquid film flowrate are similar to those for the round tube, except that for the entrained liquid flowrate there are some extra terms to the equation:

(i) There is a term to account for turbulent gas phase mixing between adjacent subchannels. This is accounted for by a term which has the form of a concentration difference between the subchannels multiplied by a mass-transfer coefficient and the area available for transfer. This representation was used as it is similar to the equation used for deposition.

(ii) There are two terms to account for the flow of entrained liquid carried around the bundle by cross flow of gas. Two terms are necessary because if a particular gas cross flow is reversed, then the subchannel from which the flow originates (the donor subchannel) has a different concentration of entrained liquid drops in the gas phase. It is assumed here that the cross flow of gas carries liquid droplets with it, and that the droplets adopt the same cross flow velocities as the gas. It is certain that the droplets do not behave in this way, but the effect of their actual behaviour is not known.

The equations then are

$$\frac{\mathrm{d}W_{LEi}}{\mathrm{d}z} = S_{Si}(E_i - D_i) + \sum_{j=1}^{N} k_{cij} S_{Fij}(C_j - C_i) n_{ji} \quad \text{turbulent mixing between subchannels} \qquad [10]$$

$$+ \sum_{j=1}^{N} a_{ij} \frac{W_{LEi}}{W_{Gi}} J_{Gji} n_{ji} + \sum_{j=1}^{N} b_{ij} \frac{W_{LEj}}{W_{Gj}} J_{Gji} n_{ji} \quad \text{Transfer of entrained liquid between subchannels due to gas crossflow}$$

where the symbols have the following meaning

W_{LEi} entrained liquid flow rate in each subchannel of type i;
S_{Si} solid surface per unit length in each subchannel of type i;
E_i entrainment rate from solid surface in a subchannel of type i;
D_i deposition rate from gas core on to solid surface in a subchannel of type i;
N number of subchannel types;
k_{cij} mass-transfer coefficient for turbulent interchange of entrained drops between subchannels of type i and j;
S_{Fij} area of boundary in the fluid per unit length between each subchannel of type i and each subchannel of type j;
C_i concentration of entrained droplets in the gas core of a subchannel of type i;
n_{ij} number of subchannels of type i bordering on each subchannel of type j, n_{ij} is thus zero if subchannel types i and j are not adjacent. Note that n_{ij} is not necessarily equal to $-n_{ji}$;

W_{Gi} gas flowrate in each subchannel of type i;

J_{Gij} the crossflow of gas from each subchannel of type i to each subchannel of type j per unit length of the bundle, J_{Gij} is zero if subchannel types i and j are not adjacent. Note that $J_{Gij} = -J_{Gji}$

a_{ij}, b_{ij} constants taking the value of zero or unity;

when $J_{Gij} > 0$ then $a_{ij} = 1, b_{ij} = 0$;

when $J_{Gij} < 0$ then $a_{ij} = 0, b_{ij} = 1$;

and when $J_{Gij} = 0$ then $a_{ij} = 0, b_{ij} = 0$.

$$\frac{dW_{LFi}}{dz} = S_{Si}\left(D_i - E_i - \frac{\phi_i}{\lambda}\right) \quad [11]$$

where ϕ_i is the heat flux on the solid surface of a subchannel of type i. There is one equation like [10], and another like [11] for each type of subchannel.

3.2 *Entrainment and deposition*

To integrate[10] and [11] it is again necessary to be able to calculate the deposition and entrainment rates.

The deposition rate d_i, by analogy with [4], can be written as

$$D_i = k_i C_i, \quad [12]$$

where k_i is the mass-transfer coefficient for deposition for subchannels of type i.

Similarly the entrainment rate E, by analogy with [8], can be written as

$$E_i = k_i C_{Ei}, \quad [13]$$

where C_{Ei} is the equilibrium concentration of droplets in subchannels of type i. C_{Ei} is again a function of $\tau_i m_i/\sigma$, where τ_i and m_i are the interfacial shear stress and the mean liquid film thickness in subchannels of type i. τ_i and m_i are evaluated in the same way as for a round tube, see section 2.3. In order to use the same equations as before the hydraulic mean diameter d_{0i} (4x cross sectional area/wetted perimeter) for a subchannel is evaluated and used in place of d_0.

3.3 *Pressure gradients*

If it is assumed that the crossflow pressure drops are small compared to the axial pressure drops, then it can be said that the total axial pressure gradient in all subchannel types must be equal at any axial position. This condition can be satisfied by continually redistributing some of the gas phase with its associated entrained liquid drops. This redistribution causes the cross flow gas flows J_{Gij}.

The total axial pressure gradient in each subchannel can be evaluated, it is the sum of the frictional. gravitational and accelerational pressure gradients

(i) The frictional pressure gradient can be calculated from the hydraulic mean diameter and the interfacial shear stress if it is assumed that the interfacial shear stress is almost equal to the wall shear stress. This is quite a good assumption as the liquid films are very thin.

(ii) The gravitational pressure drop can be calculated if the void fraction α_i in a subchannel of type i is known. This can be calculated because

α_i = fraction of cross section occupied by gas

= (1 − fraction occupied by liquid film) (volume fraction of the core flow which is gas)

$$\simeq \left(1 - \frac{4m_i}{d_{0i}}\right)\left[\frac{W_{Gi}/\rho_G}{(W_{Gi}/\rho_G)+(W_{LEi}/\rho_L)}\right]. \quad [14]$$

The term within the square brackets has been derived using an assumption of homogeneous flow in the core.

(iii) The accelerational pressure gradient can be found from the changes in the momentum flux in a subchannel. In order to calculate the momentum flux it is necessary to know the actual velocities of each component (gas, liquid film or entrained liquid) of the flow. The mean velocity of the liquid in the film in each subchannel U_{LFi} can be calculated as the film flowrate W_{LFi} and the mean film thickness m_i are known

$$U_{LFi} = \frac{W_{LFi}}{S_{Si} m_i \rho_L}. \quad [15]$$

The mean velocity of the entrained liquid U_{LEi} and the gas U_{Gi} in each subchannel is again calculated on the basis of homogeneous flow in the core, and if $m_i \ll d_{0i}$.

$$U_{LEi} = U_{Gi} = \frac{(W_{LEi}/\rho_L)+(W_{Gi}/\rho_G)}{A_i}, \quad [16]$$

where A_i is the cross sectional area of each subchannel of type i.

In the calculation of the redistributed flows, it was assumed, for iterative purposes only, that the total axial pressure gradient in each subchannel is linearly dependent upon the mass flowrate of gas in that channel. If the redistribution is repeated the procedure converges quite rapidly, and after three or four iterations the total axial pressure gradients only differ by about 0.1%.

3.4 *Calculation of the gas cross flow rates*

By a mass balance on the gas phase in each subchannel of type i, it can be shown that

$$\frac{dW_{Gi}}{dz} = \frac{S_{Si}\phi_i}{\lambda} + \sum_{j=1}^{N} J_{Gji} n_{ji}. \quad [17]$$

Only $N-1$ of these N equations are independent, the N^{th} equation is merely an expression of the overall heat balance. thus the $N-1$ equations are only soluble if there are $N-1$ non-zero values J_{Gij}. This will be true in some rod bundles, but not in others. Bowring (1968) has stated that the number, N_J of non-zero values of J_{Gij} is given by

$$N_J = N - 1 + N_L \quad [18]$$

where N_L is the number of independent loops in the subchannel network. The concept of loops is illustrated by a 37 rod bundle in figures 7 and 8. This has been divided into subchannels of 7 types, see figure 7. Figure 8 shows how these subchannels are connected. Subchannel type 1 is connected only to type 2, type 2 is connected to type 1 and type 3 (connection to other subchannels of type 2 are not shown because J_{G22} must be zero) and so on. The loops can be seen in figure 8; there are three loops but only two of them are independent.

(i) subchannel types 3, 4 and 5;
(ii) subchannel types 4, 5, 7 and 6;
(iii) subchannel types 3, 4, 6, 7 and 5.

It should be noted that with $N_J = 8$, $N = 7$, and $N_L = 2$, [18] is satisfied.

A physically reasonable assumption about the flow around these loops is that there is no net

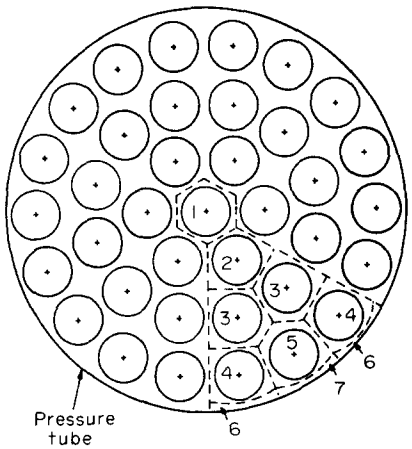

Figure 7. Thirty-seven-rod bundle.

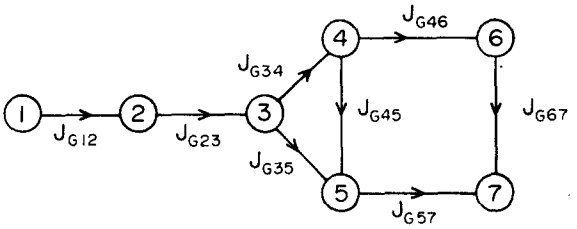

Figure 8. Subchannel connections for 37-rod bundle shown in figure 7.

circulation around a loop, hence for each independent loop there is an equation

$$\sum_{\text{loop}} J_{Gji} n_i n_{ji} = 0 \qquad [19]$$

where n_i is the number of subchannels of type i.

There are now sufficient equations for all the non-zero values of J_{Gij} to be obtained.

3.5 *Boundary conditions*

As for the round tube case the integration was started at the axial position where the quality was equal to 1% and there the fraction of liquid entrained was assumed to be 99%.

There must also be assumed some initial distribution of gas, liquid film and entrained liquid between the subchannel types. This initial distribution was calculated from the following assumptions

(i) For every subchannel type $W_{LFi}\, S_{Si}$ has the same value;

(ii) The concentration of droplets, C_i is the same in every subchannel type;

(iii) The total axial pressure drop is the same in every subchannel. The friction and gravitational components are calculated as before from τ_i and m_i (see Section 3.3). The accelerational component is approximated by the average accelerational pressure gradient between a quality of zero and a quality of 1% where the calculation is started. This average is calculated on the basis of a homogeneous flow assumption.

3.6 *Integration method and calculation scheme*

It is again necessary to use an implicit method to integrate the $2N$ equations similar to [10] and [11]. An implicit method due to Gear (1968) was found to give accurate results, an overall mass balance providing a check on the solution. Again the integration was continued until one of the film flowrates was equal to zero indicating that dryout had occurred or until the end of the channel was reached. The dryout power is then the lowest value of the total channel power which will cause dryout to occur in the channel.

Figure 9 shows a schematic diagram of the general scheme of the calculation; this diagram is drawn for simplicity for a simple explicit integration scheme.

4. RESULTS

The procedure outlined above was used to calculate the dryout power in a number of types of channel. Three examples are given here.

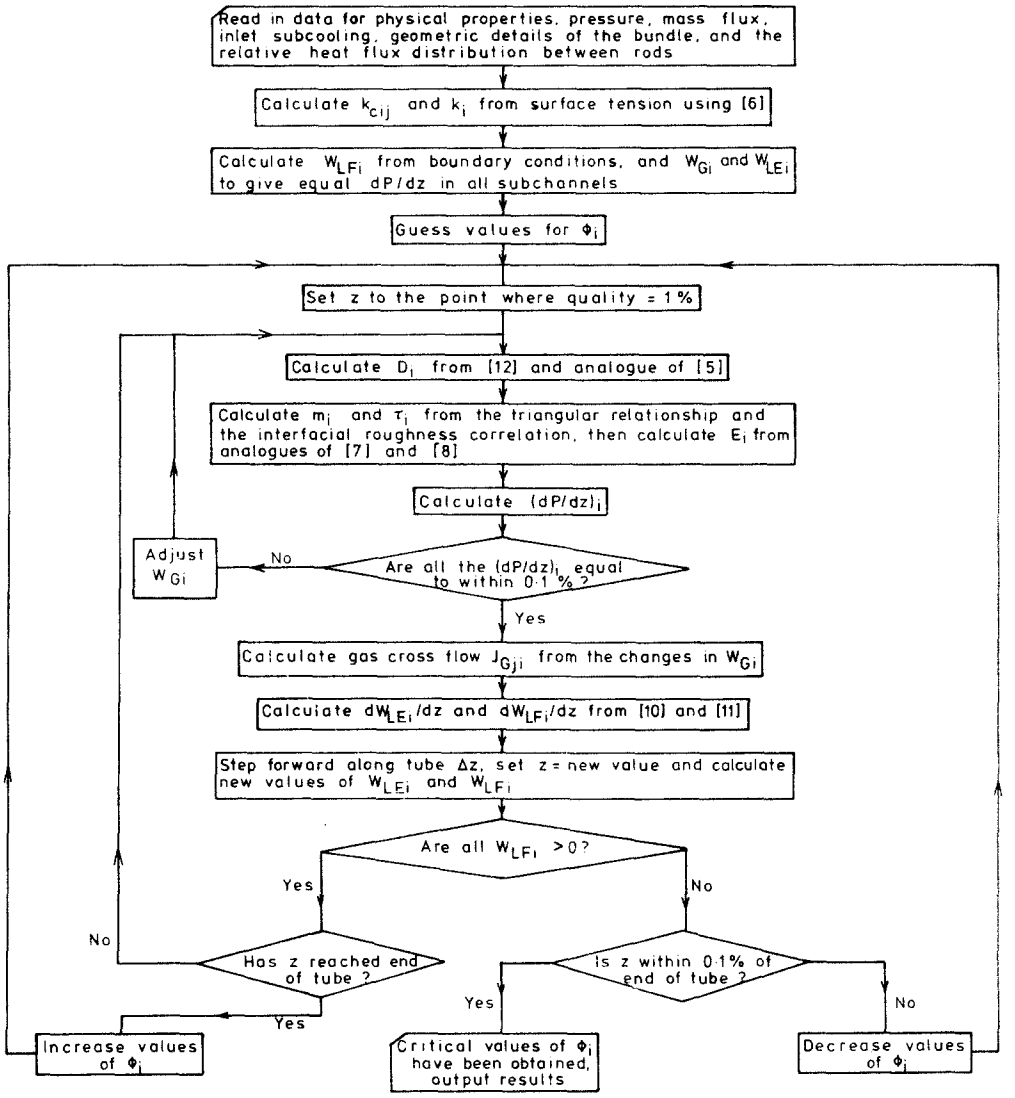

Figure 9. General scheme of calculation of dryout heat fluxes in a rod bundle.

It should be noted that in these examples the correlations for entrainment, deposition, and the liquid film characteristics (τ and m) are entirely unchanged from those previously employed by Whalley *et al.* (1974) for round tubes, and described earlier. For any particular calculation all the values of k_{cij} and k_i were equal and were given by the deposition coefficient-surface tension relation [6] illustrated in figure 5. Although the calculations described here will also yield values of pressure drop and void fraction, only comparisons of dryout power or dryout quality are described here.

4.1 *Thirty-seven-rod bundle in a circular pressure tube*

A bundle similar to that shown in cross section in figure 7 is used in the prototype Steam Generating Heavy Water Reactor at Winfrith. The central 'rod' is unheated, and is actually a tube which forms part of the emergency core cooling system. Results of some in-reactor dryout tests have been reported by Redpath (1974). The flowrate in an instrumented channel was reduced until dryout occurred. In the experiments simulated the coolant was light water at 62 bars and the heated length of channel was 3.66 m. The fuel rods all had the same enrichment so that the heat flux was greatest on the outer ring of rods. The effect of the axial heat flux profile and the circumferential heat flux variation around a rod (pin tilt) were neglected as these are not thought to affect the dryout power greatly.

Figure 10 shows the calculated results together with a curve which was fitted by Redpath through the experimental data. Dryout was predicted to occur on the outer ring of rods, and this was where it was found to occur in the experimental study. It should be noted that there was some doubt as to whether the bundle was mounted concentrically in the pressure tube.

A comparison has also been made between unpublished data for the dryout power in an electrically heated bundle of this geometry with the calculated power. The root mean square error in the calculated power was approximately 7.5% for a series of experiments where the pressure varied from 15 to 68 bars, and the mass flux from 680 to 2380 kg/m^2 sec.

4.2 *Variable geometry seven-rod bundles cooled by Freon* 12*

Kinneir *et al.* (1969) have reported measurements of dryout power in a seven rod bundle, where all seven rods are heated, cooled by Freon 12 at a pressure of 10.7 bars. The geometry of the bundle was varied so that the gap between the rods was varied, the outer six rods were always at the vertices of a regular hexagon, with the seventh rod at the centre of the hexagon (see figure 11). In one set of tests the outer rods were touching the centre rods, in another they were touching the pressure tube—positions intermediate between these extremes were also studied. The heated length of the channel was 3.66 m.

Experimental and calculated dryout powers as a function of the gap between the outer and the centre rod are shown in figure 12. The agreement between experimental and calculated values is quite reasonable until the gap between the rods becomes very small. Figure 13 shows the seven rod bundle when the gap is equal to zero. It can be seen that for this situation the subchannels shown are quite inappropriate for the situation, as subchannel type 2 has been divided into distinct and separate parts.

It was found experimentally that when the gap was small dryout occurred on the centre rod, and when the gap was large it occurred on an outer rod. A similar trend was found in the calculated results except that the change from dryout on the centre rod to dryout on an outer rod occurred at slightly too large a gap.

4.3 *Sixteen-rod bundles in a square channel*

Janssen *et al.* (1969) have studied a 16-rod bundle in a square channel, shown in cross-section in figure 14. It can be seen from this figure that the corner subchannels are of a peculiar shape. It is probable that liquid will collect in the corners, and so make the film flowrate larger than would be otherwise expected. These effects were not taken into consideration here. The

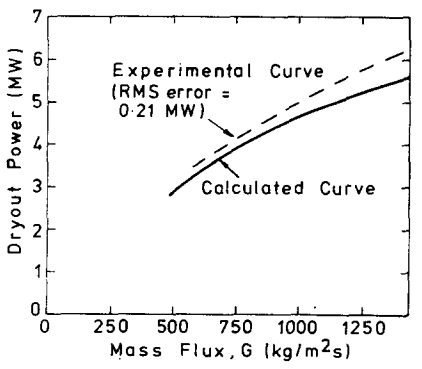

Figure 10. Experimental and calculated results for dryout power in a 37-rod bundle, inlet subcooling = 63 kJ/kg.

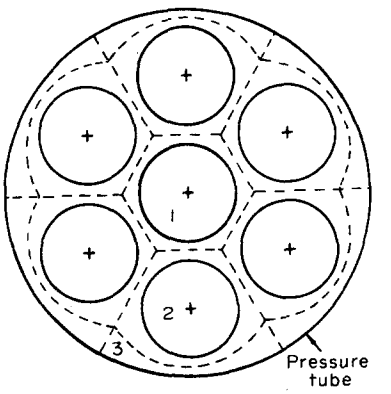

Figure 11. Seven-rod bundle used in Freon tests by Kinneir *et al.* (1969).

*A registered Trade Mark of DuPont Ltd.

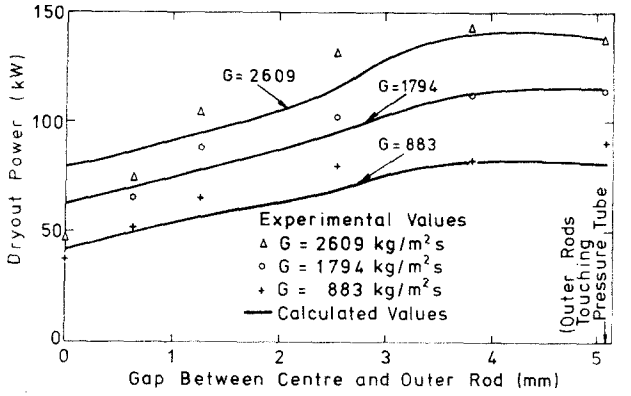

Figure 12. Experimental and calculated dryout powers for a 7-rod bundle cooled by Freon 12 for various rod separations. Experimental results from Kinneir *et al.* (1969), inlet subcooling = 11.6 kJ/kg.

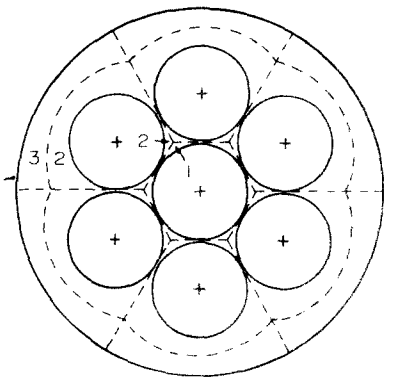

Figure 13. Subchannels used for 7-rod bundle when outer rods are touching centre rod.

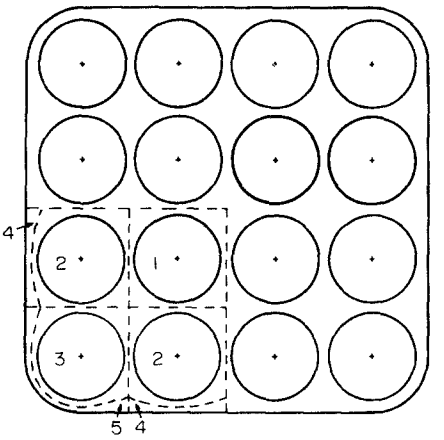

Figure 14. Sixteen-rod bundle.

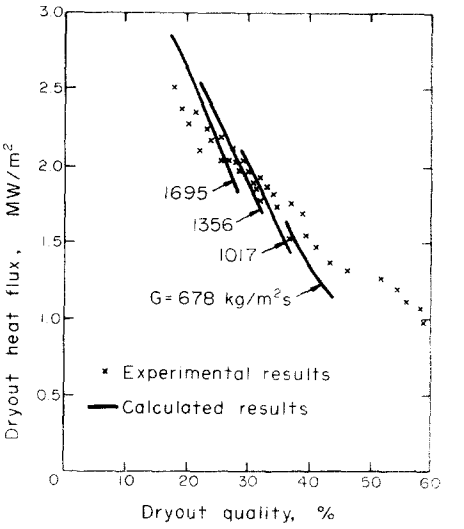

Figure 15. Experimental and calculated variation of dryout heat flux with dryout quality for 16-rod bundle. Experimental points from Janssen *et al.* (1969).

rods, in the experiments simulated, were heated uniformly so that the heat flux on every rod was equal. The heated length of the channel was 1.83 m and it was cooled by water at a pressure of 69 bars. The maximum subcooling of the water at the start of the heated length was large—over 400 kJ/kg in some cases. This has the result that the length of channel where the quality is greater than zero is sometimes less than 1 m. It was found by Whalley *et al.* (1974) that the calculated dryout power for short boiling lengths was not very accurate for a straight tube.

Janssen *et al.* plotted their results in the form of critical heat flux vs dryout quality. They found that their experimental results fell approximately on a single curve even for quite wide ranges of inlet subcooling. Figure 15 shows the experimental and calculated results. For each of the four mass velocities used in the calculation, the inlet subcooling was varied over the range 0 to 400 kJ/kg.

Both theoretically and experimentally it was found that dryout always occurred on a corner rod.

5. CONCLUSIONS

A method for calculating the dryout power in a rod bundle has been described, and a number of results presented. From these results it can be seen that the method gives a reasonable estimate of the dryout power except when, either the boiling length is very short, or the use of rod centred subchannels is inappropriate. It should be noted again that the correlations used in the calculation method, and the constants necessary as input data, are all exactly the same as are used for calculating the dryout behaviour of a single round tube. No optimisation of the constants of the model for the rod bundle has been necessary.

The present calculation method is subject to a number of restrictions, and it is worth noting which of these restrictions are simple to remove. There is first a group of restrictions, the removal of which would present no great difficulty.

(i) The fluid physical properties are assumed constant along the channel. The physical properties could be allowed to vary by performing an overall enthalpy balance on the elemental length δz in figure 4. In this way the vaporisation rate due to both the imposed heat flux and the flashing of the liquid could be calculated.

(ii) There is no variation of the heat flux along the channel. This restriction can be removed by putting ϕ_i in [11] to be a function of the axial position z.

(iii) The cross flow pressure drops are neglected; these could be taken into account and would mean that the pressure would no longer be the same in each subchannel at a given axial position z.

(iv) No sparge flows in the bundle must be present. In the Steam Generating Heavy Water Reactor water is continuously sprayed into the bundle at a low flowrate by the emergency core cooling system. The effect of such a sparge flow would be to increase W_{LEi} and W_{LFi} at the axial spray positions.

There is a second group of restrictions, the removal of which would be more difficult.

(i) The flow is assumed to be steady. Transient flow in a tube has been studied by Whalley *et al.* (1975), but the extension of this work to the rod bundle geometry presents a considerable computational problem.

(ii) Pin tilt (the variation of heat flux circumferentially round a rod) cannot be simulated. This would lead to variations in liquid film characteristics around the rod circumference.

(iii) There is no representation of any effects caused by grids and spacers in the bundle. Obviously support grids will affect the liquid film in some way, but it is not clear in detail what will happen to the film as it passes over or through a grid.

Finally, it must be remembered that this calculation method is based on a model of annular flow, and so no representation of any phenomenon such as subcooled dryout is possible.

REFERENCES

ARMAND, A. A. 1946 The resistance during the movement of a two phase flow system in horizontal pipes. *Isv. Vseoyuz. Teplotekn. Inst.* **1**, 16–23.

BENNETT, A. W., HEWITT, G. F., KEARSEY, H. A., KEEYS, R. K. F. & LACEY, P. M. C. 1965 Flow visualisation studies of boiling at high pressure. U.K.A.E.A. report AERE-R4874.

BENNETT, A. W., HEWITT, G. F., KEARSEY, H. A., KEEYS, R. K. F. & PULLING, D. J. 1967 Studies of burnout in boiling heat transfer. *Trans. Instn Chem. Engrs* **45**, T319–T333.

BERGLES, A. E., ROOS, J. P. & BOURNE, J. G. 1968 Investigation of boiling flow regimes and critical heat flux. U.S.A.E.C. (Dynatech Corporation) report NYO-3304-13.

BERKOWITZ, L., BERTOLETTI, S., LESAGE, J., PETERLONGO, G., SOLDAINI, G. & ZAVATTARELLI, R. 1960 Results of wet steam cooling experiments: pressure drop, heat transfer and burnout measurements with round tubes. C.I.S.E. report R-27.

BOWRING, R. W. 1967 HAMBO—a computer program for the subchannel analysis of the

hydraulic and burnout characteristics of rod clusters, Part I, General description. U.K.A.E.A. report AEEW-R524.

BOWRING, R. W. 1968 HAMBO—a computer program for the subchannel analysis of the hydraulic and burnout characteristics of rod clusters, Part II, The equations. U.K.A.E.A. report AEEW-R582.

BUTTERWORTH, D. 1968 Air–water climbing film flow in an eccentric annulus. Int. symposium on Research in Co-current Gas–Liquid Flow, University of Waterloo, Ontario, Paper B2.

COUSINS, L. B., DENTON, W. H. & HEWITT, G. F. 1965 Liquid–mass transfer in annular two phase flow. *Proc. Two-Phase Flow Symposium*, University of Exeter, Paper C4.

COUSINS, L. B. & HEWITT, G. F. 1968*a* Liquid phase mass transfer in annular two phase flow: droplet deposition and liquid entrainment. U.K.A.E.A. report AERE-R5657.

COUSINS, L. B. & HEWITT, G. F. 1968*b* Liquid phase mass transfer in annular two phase flow: radial liquid mixing. U.K.A.E.A. report AERE-R5693.

GASPARI, G. P., HASSID, A. & VANOLI, G. 1970 Some considerations on critical heat flux in rod clusters in annular dispersed vertical upward two phase flow. *4th Int. Heat Transfer Conference*, Paris, Paper B6.4.

GASPARI, G. P., HASSID, A. & LUCCHINI, F. 1974 A rod-centred subchannel analysis with turbulent (enthalpy) mixing for critical heat flux prediction in rod clusters cooled by boiling water. *5th Int. Heat Transfer Conference*, Tokyo, Paper B6.12.

GEAR, C. W. 1968 The automatic integration of stiff ordinary differential equations. Proceedings I.F.I.P. Congress.

GILL, L. E., HEWITT, G. F. & LACEY, P. M. C. 1964 Sampling probe studies of the gas core in annular two-phase flow—II. Studies of the effect of phase flow rates on phase and velocity distribution. *Chem Engng Sci.* **19**, 665–682.

GILL, L. E., HEWITT, G. F. & ROBERTS, D. N. 1969 Studies of the behaviour of distrubance waves in annular flow in a long vertical tube. U.K.A.E.A. report AERE-R6012.

HEWITT, G. F. 1961 Analysis of annular two-phase flow: application of the Dukler analysis to vertical upward flow in a tube. U.K.A.E.A. report AERE-R3680.

HEWITT, G. F. & HALL-TAYLOR, N. S. 1970 *Annular Two Phase Flow.* Pergamon Press, Oxford.

HEWITT, G. F., KEARSEY, H. A., LACEY, P. M. C. & PULLING, D. J. 1965 Burnout and nucleation in climbing film flow. *Int. J. Heat Mass Transfer* **8**, 793–814.

HUTCHINSON, P. & WHALLEY, P. B. 1973 A possible characterisation of entrainment in annular flow. *Chem. Engng Sci.* **28**, 974–975.

JANSSEN, E. & KERVINEN, J. A. 1964 Two phase pressure drop in straight pipes and channels with water–steam mixtures at 600 to 1400 psia. General Electric report GEAP-4616.

JANSSEN, E., SHRAUB, F. A., NIXON, R. B., MATZNER, B. & CASTERLINE, J. F. Sixteen-rod heat flux investigation: steam–water at 600 to 1400 psia in *Two-Phase Flow and Heat Transfer in Rod Bundles*, Am. Soc. Mech. Engrs.

KEEYS, R. K. F., RALPH, J. C. & ROBERTS, D. N. 1970 Liquid entrainment in adiabatic steam–water flow at 500 and 1000 psia (34.5 and 69 bars). U.K.A.E.A. report AERE-R6293.

KINNEIR, J. H., HERON, R., STEVENS, G. F. & WOOD, R. W. 1969 Burn-out power and pressure drop measurements on 12 ft. 7-rod clusters cooled by Freon 12 at 155 psia. European Two-Phase Flow Group Meeting, Karlsruhe.

REDPATH, W. 1974 Winfrith S.G.H.W.R. in-reactor dryout tests. J. Br. Nucl. Energy Soc. **13**, 87–97.

ROWE, D. S. 1967 Cross-flow mixing between parallel flow channels during boiling, Part I COBRA computer program for constant boiling in arrays. Battelle Northwest report BNWL-371.

ROWE, D. S. 1970 COBRA-II, a digital computer program for thermal hydraulic subchannel analysis of rod bundle nuclear fuel elements. Battelle Northwest report BNWL-1229.

ROWE, D. S. 1972 COBRA-III, a digital computer program for the steady state and transient

thermal hydroaulic analysis of rod bundle nuclear fuel elements. Battelle Northwest report BNWL-B-82.

ROWE, D. S. 1973 COBRA-IIIc a digital computer program for the steady state and transient thermal analysis of rod bundle nuclear fuel elements. Battelle Northwest report BNWL-1695.

SINGH, K., ST. PIERRE, C. C., CRAGO, W. A. & MOECK, E. O. 1969 Liquid film flowrates in two-phase flow of steam and water at 1000 psia. *A.I.Ch.E.Jl.* **15**, 51–56.

TRUONG QUANG MINH & HUYGHE, J. D. 1965 Some hydrodynamic aspects of annular dispersed flow, entrainment and film thickness. Proc. of Two-Phase Flow symposium, University of Exeter, Paper C2.

TURNER, J. M. & WALLIS, G. B. 1965 An analysis of the liquid film in annular flow. U.S.A.E.C. (Dartmouth College) report NYO-3114-13,

WALLIS, G. B. 1970 Annular two-phase flow: part 2, additional effects. *J. Basic Engng* **92**, 73–82.

WEISMAN, J. & BOWRING, R. W. 1975 Methods for detailed thermal and hydraulic analysis of water cooled reactors. *Nucl. Sci. Engng* **57**, 255–276.

WHALLEY, P. B., HUTCHINSON, P. & HEWITT, G. F. 1974 The calculation of critical heat flux in forced convection boiling. 5th Int. Heat Transfer Conference, Tokyo, Paper B6.11.

WHALLEY, P. B., HUTCHINSON, P. & HEWITT, G. F. 1975 Prediction of annular flow parameters for transient conditions and for complex geometries. European Two-Phase Flow Group Meeting, Haifa, Israel.

WILLIAMS, C. L. & PETERSON, A. C. 1975 Flow patterns in high pressure two phase flow—a visual study of water in a uniformly heated 4-rod bundle. Westinghouse report WAPD-TM-1199.